arXiv:astro-ph/0206208v1 13 Jun 2002

Extended HI spiral structure and the figure rotation of triaxial dark halos

Kenji Bekki
School of Physics, University of New South Wales, Sydney 2052, Australia

and

Kenneth C. Freeman
Mount Stromlo and Siding Spring Observatories, The Australian National University, Private Bag, P.O. Weston Creek, ACT 2611, Australia

ABSTRACT

The HI disk of the blue compact dwarf (BCD) galaxy NGC 2915 extends to 22 optical scalelengths and shows spiral arms reaching far beyond the optical component. None of the previous theories for spiral structure provide likely explanations for these very extended spiral arms. Our numerical simulations first demonstrate that such large spiral arms can form in an extended gas disk embedded in a massive triaxial dark matter halo with slow figure rotation, through the strong gravitational torque of the rotating halo. We then show that the detailed morphological properties of the developed spirals and rings depend strongly on the pattern speed of the figure rotation, the shape of the triaxial halo, and the inclination of the disk with respect to the plane including the triaxial halo's long and middle axes. These results strongly suggest that the dark matter halo of NGC 2915 is triaxial and has figure rotation. Based on these results, we also suggest that dynamical effects of triaxial halos with figure rotation are important in various aspect of galaxy formation and evolution, such as formation of polar ring galaxies, excitation of non-axisymmetric structures in low surface-brightness galaxies, and gas fueling to the central starburst regions of BCDs.

Subject headings: galaxies: dwarf — galaxies: formation — galaxies: ISM — galaxies: kinematics and dynamics — galaxies: spiral

1. Introduction

To understand the distribution and the nature of dark matter in galaxies and dynamical effects of dark matter halos on galaxies has been a longstanding and remarkable problem in galactic astronomy (e.g., Trimble 1987; Ashman 1992; Salucci & Persic 1997). Detailed analysis of rotation curves in variously different galaxies have played a major role in revealing the radial distributions of dark matter halos in galaxies (Salucci & Persic 1997 for a review). Recently high-resolution rotation curve studies for low surface brightness galaxies and dwarfs have extensively discussed whether or not the radial density profiles of dark matter halos predicted from cold dark matter (CDM) models (Navarro, Frenk, & White 1996) are consistent with the observationally inferred profiles (e.g., de Blok et al. 2001; van den Bosch & Swaters 2001).

Several attempts have been so far made to reveal the *shapes* (e.g., the degree of oblateness or triaxiality) of dark matter halos in galaxies (e.g., Trimble 1987; Ashman 1991). Following the early attempts to use the kinematics of polar rings for deriving the three dimensional mass distributions of galaxies (Schweizer et al. 1983; Whitmore et al. 1987), Sackett & Sparke (1990) tried to give strong constraints on the shape of a dark matter halo in polar ring galaxy NGC 4650A by investigating both a rotation curve of a polar ring component and that of a planner disk one. They concluded that the best modeled flattening of the dark halo in NGC 4650A is somewhere between E3 and E7. Franx, van Gorkom, & de Zeeuw (1994) analyzed both the geometry and the velocity of the HI gas ring of IC 2006 and found a nonsignificant ellipticity of the gravitational potential ($\sim 0.012 \pm 0.026$).

Furthermore, Olling (1995) found that the thickness of the HI gas disk extending beyond the Holmberg radius in a galaxy is sensitive to the flattening of the dark matter halo and proposed that the high resolution HI studies on the flaring of the outer gas layers in nearby galaxies enables us to determine the shape of the dark matter halos. By comparing numerical simulations of dynamical evolution of the Sagittarius dwarf with observations on the detailed spatial distribution of the 75 Galactic halo stars, Ibata et al. (2001) suggested that the Galactic dark halo is most likely almost spherical in the Galactocentric distance 16 $< R <$ 60 kpc. Based on the structural and kinematic properties of the Galactic luminous A-type stars revealed by Hipparcos data (ESA, 1997), Crézé et al. (1998) argued that there are strong lower limits on the scaleheight of any flattened component of the galactic dark halo.

Although the radial density profiles and the shapes of dark matter halos have been extensively discussed by many authors, their *rotational properties* have been less discussed. Based on the detailed analysis of structure and kinematics of the very extended HI disk around NGC 2915, Bureau et al (1999) first suggested that the observed spiral-like

structures in the HI disk can be formed by a triaxial halo with figure rotation. They furthermore pointed out that the slow pattern speed of the figure rotation inferred from the kinematics and density distribution of the HI gas is consistent with the pattern speeds of rotating triaxial dark halos seen in CDM simulations analysed by Pfitzner (2000). However, it is unclear whether a triaxial dark halo with figure rotation is really responsible for the observed extended spiral structures in NGC 2915, because of the lack of numerical studies of gas dynamics in the gravitational potentials of triaxial halos with figure rotation.

The purpose of this Letter is to demonstrate how non-axisymmetric structures (e.g. spirals and bars) can be formed in a gas disk well outside the optical radius of a galaxy embedded in a massive triaxial dark matter halo with figure rotation. We particularly investigate how morphological evolution of outer gas disks depends on the structure of the triaxial halos, the pattern speeds of the figure rotation, and the physical properties of the disks (e.g. inclination of the disks with respect to the halo and gaseous mass and temperature).

2. Model

We consider an extended uniform gas disk of a dwarf galaxy embedded by a triaxial dark matter halo with figure rotation. We adopt TREESPH codes described in Bekki (1997) for hydrodynamical evolution of galaxies and thereby investigate the dynamical evolution of the gas disk under the triaxial dark halo. All of the following physical parameters are based on observations on NGC 2915 by Meurer et al (1996) and Bureau et al (1999). The observed HI extent (the radius within which the HI column density is observed to be larger than 5×10^{19} cm^{-2}) is ~ 15 kpc, which is about 5 times larger than the $B-$band Holmberg radius (~ 3 kpc) of the host NGC 2915. This unusually extended HI gas is modeled as an uniform thin gas disk with the size (represented by $R_{\rm g}$) of 15 kpc and the mass ($M_{\rm g}$) of 10^8 $M_\odot$. The gas disk with uniform radial density distribution is represented by 20K SPH particles and each gas particle is first placed in the x-y plane and given its circular velocity (determined by the dark matter halo) at its radius. The gas disk is then inclined by θ degree with respect to the x-y plane. An isothermal equation of state is used for the gas with a temperature of 1.2×10^3 K corresponding to a sound speed of 4 km s^{-1} (~ 0.075 times the virial velocity of the system).

This extended and inclined gas disk is assumed to be dynamically affected *only* by a massive dark matter halo with the mass $M_{\rm DM}$ of 10^{10} $M_\odot$, because the mass of the central stellar components of the dwarf (with $M_{\rm B} = -15.9$ mag) is negligibly small compared with that of the dark matter. We adopt the density distribution of the NFW halo (Navarro,

Frenk & White 1996) suggested from CDM simulations:

$$\rho(r) = \frac{\rho_0}{(r/r_{\rm s})(1+r/r_{\rm s})^2}, \tag{1}$$

where ρ_0 and $r_{\rm s}$ are the central density and the scale length of a dark halo, respectively. It is still controversial whether dark matter halos have constant density cores instead of inner steep cusps described above (e.g., van den Bosch & Swaters 2001), so we also ran simulations in halos with constant density cores, as in Salucci & Burkert (2000). We find that the resulting structures are essentially the same as those for the NFW profiles, so they will not be further discussed here. The scale length $r_{\rm s}$ is treated as a parameter, whereas ρ_0 is chosen such that the total mass of a dark halo within the disk radius $R_{\rm g}$ is $M_{\rm DM}$ ($= 10^{10}$ $M_\odot$) for a given $r_{\rm s}$. We only present the results of models with $r_{\rm s} = 0.75$ kpc, because our results depend only weakly on $r_{\rm s}$.

We take the isodensity surfaces of the dark halo to be triaxial ellipsoids on which the Cartesian coordinates (x,y,z) satisfy the following condition (Binney & Tremaine 1987):

$$m^2 \equiv \frac{x^2}{a^2} + \frac{y^2}{b^2} + \frac{z^2}{c^2} = constant, \tag{2}$$

where a, b, and c are the parameters which determine the two axis ratios of a triaxial body (i.e., long to short and long to middle). In the present study, a is set to be 1 and the long-axis is initially coincident with the x axis. Accordingly b (≤ 1) and c (≤ 1) are free parameters which determine the shapes of triaxial dark matter halos. The triaxial halo is assumed to be rotating as a solid body with the pattern speed of $\Omega_{\rm p}$. The figure rotation of triaxial dark matter halos and their typical pattern speeds have been already observed in high-resolution collisionless CDM simulations by Pfitzner (2000); see some of the results in Bureau et al. (1999).

By changing the parameters $R_{\rm g}$, θ, b, c, and $\Omega_{\rm p}$, we investigate morphological evolution of extended gas disks and its dependence on shapes and rotational properties of triaxial halos. The parameter values of $R_{\rm g}$, θ, b, c, and $\Omega_{\rm p}$ are 15 kpc, 30°, 0.8, 0.6, and 3.84 km s^{-1} kpc^{-1}, respectively, in *the standard model* (Model 1) which shows typical behaviors of gaseous response to triaxial halos and thus described in detail. The two key parameters of spiral arm formation are the Toomre's X and Q parameters (Toomre 1964, 1981) and these are described as

$$X(r) \equiv \frac{r\kappa(r)^2}{2\pi G m \mu(r)}, \tag{3}$$

where $\kappa(r)$, m, $\mu(r)$ are the epicyclic frequency at a given radius r, the azimuthal wavenumber of the spiral pattern, and the surface density, respectively, and

$$Q(r) \equiv \frac{v_s(r)\kappa(r)}{\pi G \mu(r)}, \tag{4}$$

where $v_s(r)$ is the sound speed of the gas. In this standard model (also in other models), X and Q are rather large in the entire disk region (e.g., 39.3 and 9.4, respectively, for $m = 2$ and $r = 15$ kpc). Such gas disks with the X and Q parameters larger than 3 required for the spiral arm formation (e.g., Binney & Tremaine 1987) are highly unlikely to form spontaneously spiral arms via the "swing amplification mechanism" (Toomre 1981). Therefore, if the spiral arms are formed in our simulations, this implies that external torque from triaxial halos plays a role in forming spiral arms in gas disks. Parameter values for each of 9 models (Model $1 - 9$) investigated in the present study are summarized in Table 1. There is only one inner Lindblad resonance (ILR) point for all models but Model 4 with retrograde pattern speed. The points of ILR ($R_{\rm ILR}$), corotation ($R_{\rm CR}$), and outer Lindblad resonance ($R_{\rm OLR}$) are given in the table for each model. In the following, our units of mass, length, and time are 10^{10} $M_\odot$ ($= M_{\rm DM}$), 15 kpc, and 2.74×10^8 yr, respectively.

3. Results

Figure 1 describes how gaseous spiral arms are formed, as the triaxial halo rigidly rotates in the standard model (Model 1). Owing to the difference in angular speed between the gas disk and the triaxial halo, the gas disk continuously suffer from the strong tidal force of the halo. As a natural result of this, two open trailing arms are gradually developed in the entire disk within 1 Gyr ($T = 4$). These two open arms quickly wind with each other to form a central high-density, ring-like structure at $R \sim 0.3$ (4.5 kpc) in our units ($T = 6$ and 8). Annular low-density gaseous regions ($0.3 \leq R \leq 0.5$ in our units) forms just outside the inner ring because of the disk's angular momentum redistribution caused by the halo's torque ($T = 10$). Thus our simulations first confirms the early suggestion (Bureau et al. 1999) that the observed unusually extended spiral arms of NGC 2915 can be due to the tidal torque of the triaxial dark matter halo with figure rotation.

Figure 2 shows that extended remarkable spiral arms can not be formed in a axisymmetric dark matter halo with figure rotation (Model 2), which strongly suggests that triaxiality is essentially important for the formation of gaseous spirals arms in dark matter halos with figure rotation. Figure 2 furthermore demonstrates that even if the self-gravity of gas is not included in the simulations, spiral arms are formed in the triaxial dark matter halo (Model 3). This implies that the physical mechanism of spiral arm formation in the present model can be essentially different from the "swing amplification mechanism" (Toomre 1981) which requires self-gravity of disks and is a standard model of spiral arm formation. Sanders & Huntley (1976) numerically investigated the dynamical response of a thin gas disk to a rigidly rotating stellar bar and found that open two-arm trailing spiral

structures can be formed owing to the tidal torque of the bar. They also demonstrated that the orientation of elliptical gas streamlines formed in the dissipative gas disk continuously rotates, and such a pattern of streamlines results in spiral density enhancement. Although their numerical methods and dynamical models are very different from ours, their proposed mechanism might well be essentially the same as that for spiral arm formation in triaxial dark matter halos with figure rotation.

Detailed morphological properties of gas disks are remarkably different between models with different shapes of dark matter halos, pattern speed of the figure rotation, sizes of initial gas disks, and the inclination angle of disks with respect to the halos. Figure 2 highlights important parameter dependences of morphological properties of gas disks. Firstly, if the figure rotation is retrograde sense with respect to the disk's rotation (Model 4), the morphological evolution of the disk is less dramatic, and consequently remarkable spiral arms can not be seen in the disk (Instead, ring-like structures can be seen in the central region). Secondly, very complicated gas rings can be formed in the model with high inclination angle (Model 5 with $\theta = 60°$). The developed outer parallelogram-like ring and inner small circular ring, both of which are actually spiral arms in the disk, are reminiscent of peculiar polar-ring galaxies NGC 660 and NGC 2685. Thirdly, more remarkable spiral arms can be formed in the model with more bar-like halo in the x-y plane (Model 6). Fourthly, spiral arm structures are likely to be less remarkable for the model with slower pattern speed of figure ration (Model 7 and 8), which confirms that not only the triaxial shape of the halo but also the figure rotation are responsible for spiral arm formation. Fifthly, it does not depend strongly on the sizes of initial gas disks whether or not spiral arms are formed. The model with compact gas disk (Model 9 with $R_{\rm g} = 0.5$) shows spiral arm structures, which implies that triaxial halos with figure rotation can greatly influence even the dynamical evolution of central galaxies.

4. Discussions and conclusions

Here are some of the implications of our results. Firstly, some of the morphological properties of polar ring galaxies result from gas response to their triaxial dark halo with figure rotation. Our models showed that the spatial distributions of gas disks can be strikingly similar to the double-ring structure observed in polar ring galaxies ESO 474 - G26 and NGC 2685 (Schweizer et al. 1983) and to a parallelogram-like structure in NGC 660 (van Driel et al. 1995). The simulated structures which appear to be polar ring components in polar ring galaxies are actually not rings but disks with spiral arms and with inner low-density gas regions. This implies that *some* polar ring components are not rings but

'polar disks' with spiral arms. NGC 4650A is observed to be such a polar disk with spiral structure (e.g., Arnaboldi et al. 1997), and accordingly might be formed by the torque of its rotating triaxial halo.

Secondly, we recall Davies's (1972) suggestion that the HVC complex C represents an outer extended Galactic spiral arm at relatively high latitude. The present simulation successfully produced extended outer gas arms in a galaxy embedded in a rotating triaxial halo. We suggest that high-density regions in the extended gaseous arms excited by the Galactic triaxial halo could be the formation sites of HVCs. Extensive discussions on the origin of HVCs based on the comparison of our simulations and HIPASS observations will be given in our forthcoming papers (Bekki & Freeman 2002).

Thirdly, the morphological properties of low surface brightness (LSB) disk galaxies can be greatly influenced by triaxial dark matter halos with figure rotation, because these LSBs are observed to be dominated by dark matter (e.g. de Blok & McGaugh 1996). Our simulations show that even a compact low-mass gas disk can be transformed into spiral arms by the gravitational torque of its rotating triaxial dark matter halo. The observed diversity in non-axisymmetric structures in LSBs (McGaugh 1992) with possibly large Toomre (1964, 1981) Q and X parameters (i.e. systems in which *spontaneous* spiral formation is highly unlikely) can be due partly to the figure rotation of their triaxial halos. Our results also imply that even in high surface brightness (HSB) galaxies, *the outer gas* can be strongly affected, if the gas is misaligned with the triaxial halos. We suggest that the observed gaseous warps in HSBs can be formed by the halos at the radius where the strong vertical restoring force of *stellar disks* drops rapidly (e.g., Briggs 1990).

Fourthly, the large-scale torques associated with the rotating triaxial halos provide a mechanism for fueling the starburst regions of BCDs by replenishing gas from their outer HI gas reservoirs.

Most dwarf irregular galaxies are observed to have HI gas extending to $\sim$ twice the Holmberg radius ($R_{\rm H}$). Some of them have gas out to $4-7 \times R_{\rm H}$ (e.g Hunter 1997). The morphologies of this extended HI gas are diverse, ranging from smooth and quiescent (e.g. NGC 6822; Roberts 1972) to spectacularly complex (e.g. NGC 4449; Bajaja et al. 1994) and with arms or blobs as in DDO 26 (Hunter & Wilcots 2002). Extended HI with spiral-like structures and arcs is seen in spirals like NGC 628 (e.g., Kamphuis & Briggs 1992). Our study strongly suggests that these apparently peculiar structures in the extended outer HI gas of galaxies can tell us something important about the shapes and the rotational properties of dark matter halos.

Systematic comparison between hydrodynamical simulations such as those presented

in this study and high-resolution morphological studies of unusually extended HI gas of galaxies might well reveal the dependence of the pattern speed of rotating triaxial dark halos on the masses, structures, and environments of galaxies. This could give useful constraints on theories of galaxies formation. Finally we would welcome high-resolution cosmological simulations which provide better statistics on the incidence of rotating figures of dark matter halos in low-mass dwarf galaxies.

We are grateful to the anonymous referee for valuable comments, which contribute to improve the present paper. K.B. acknowledges the financial support of the Australian Research Council throughout the course of this work. We would like to thank Tim de Zeeuw, Ortwin Gerhard, and Martin Bureau for helpful discussions about rotating triaxial figures.

REFERENCES

Arnaboldi, M., Oosterloo, T., Combes, F., Freeman, K. C., & Koribalski, B. 1997, AJ, 113, 585

Ashman, K. M. 1992, PASP, 104, 1109

Bajaja, E., Huchtmeier, W. K., & Klein, U. 1994, A&A, 285, 385

Bekki, K. 1997, ApJ, 483, 608

Bekki, K., & Freeman, K. C. 2002, in preparation

Binney, J., & Tremaine, S., 1987 in Galactic Dynamics.

Briggs, F. 1990, ApJ, 352, 15

Bureau, M., Freeman, K. C., Pfitzner, D. W., & Meurer, G. R. 1999, AJ, 118, 2158

Creze, M., Chereul, E., Bienayme, O., & Pichon, C. 1998, A&A, 329, 920

Davies, R. D. 1972, MNRAS, 160, 381

de Blok, W. J. G., & McGaugh, S. S. 1996, ApJ, 469, L89

de Blok, W. J. G., McGaugh, Stacy S., & Rubin, V. C. 2001, AJ, 122, 2396

ESA, 1997, The Hipparcos Catalogue, ESA SP-1200

Franx, M., van Gorkom, J. H., & de Zeeuw, T. 1994, ApJ, 436, 642

Hunter, D. A. 1997, PASP, 109, 937

Hunter, D. A., & Wilcots, E. M. 2002, prepring (astro-ph/0202149)

Ibata, R., Irwin, M, Lewis, G. F., & Stolte, A. 2001, ApJ, 547, L133

Kamphuis, J., & Briggs, F. 1992, A&A, 253, 335

McGaugh, S. S. 1992, Ph.D. thesis, Univ. Michigan

Meurer, G. R., Carignan, C., Beaulieu, S. F., & Freeman, K. C. 1996, AJ, 111, 1551

Navarro, J. F., Frenk, C. S., & White, S. D. M. 1996, ApJ, 462, 563

Olling, R. P. 1995, AJ, 110, 591

Pfitzner, D. W. 2000, in preparation

Roberts, M. S., 1972, in External Galaxies and Quasi-Stellar Object, ed. D. S. Evans (Dordrecht, Reidel) p.12

Sackett, P. D., & Sparke, L. S. 1990, ApJ, 361, 408

Salucci, P.i, & Persic, M., 1997, in Dark and Visible Matter in Galaxies, ed. M. Persic and P. Salucci ASP conf. ser. Vol. 117, p1,

Salucci, P., & Burkert, A. 2000, ApJ, 537, L9

Sanders, R. H. & Huntley, J. M. 1976, ApJ, 209, 53

Schweizer, F., Whitmore, B. C., & Rubin, V. C. 1983, AJ, 88, 909

Toomre, A. 1964, ApJ, 139, 1217

Toomre, A. 1981, in The structure and evolution of normal galaxies, ed. S. M. Fall & D. Lynden-Bell (Cambridge University Press) p111

Trimble, V. 1987, ARAA, 25, 425

van den Bosch, F. C., & Swaters, R. A. 2001, MNRAS, 325, 1017

van Driel, W. et al. 1995, AJ, 109, 942

Whitmore, B. C., McElroy, D. B., & Schweizer, F. 1987, ApJ, 314, 439

This preprint was prepared with the AAS LaTeX macros v4.0.

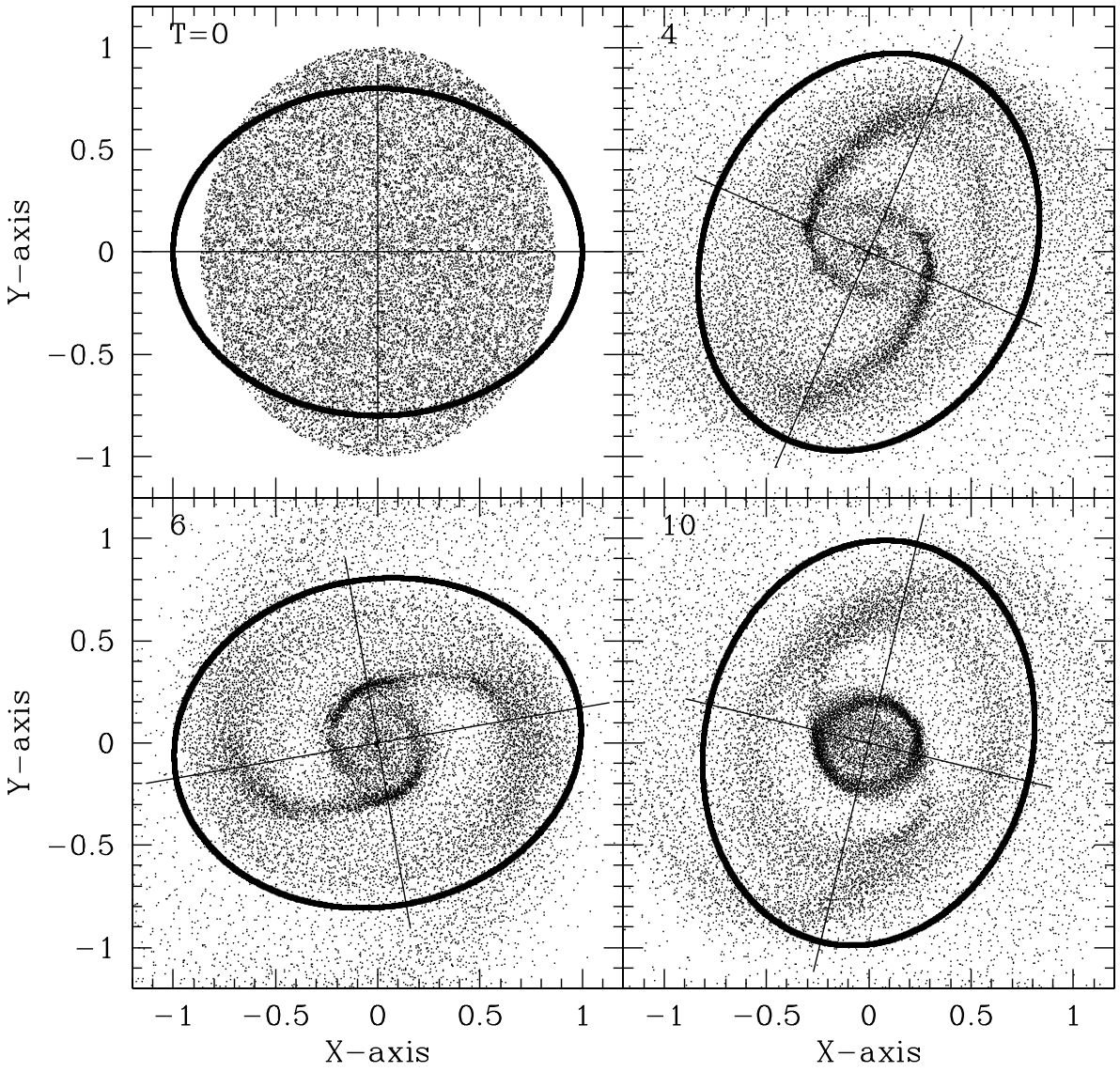

Fig. 1.— Morphological evolution of the gas disk projected onto the x-y plane for the standard model with the disk inclination (θ) of 30° with respect to the x-y plane. The time (T) indicated in the upper left corner of each frame is given in our units (2.74×10^8 yr) and each frame (2.4 in our units) measures 36 kpc on a side. The shape of the triaxial halo projected onto the x-y plane (at $R = 1.0$ in our units, corresponding to 15 kpc) is outlined by a thick solid line at each time T. Both the gas disk and the halo are assumed to rotate counter-clockwise (The spin axis of the halo is coincident with the z axis). The long and middle axes of the halo are represented by thin solid lines. Note that as the triaxial halo rigidly rotates, two open trailing spiral arms are formed at $T = 4.0$ ($\sim$ 1.1 Gyr) owing to the tidal torque of the halo. Note also that these spirals arms finally wind to form a central gaseous ring at $T = 10$ ($\sim$ 2.7 Gyr). Results of models with the lower inclination angle (0° $\leq \theta \leq$ 30°) are essentially the same as that of this model.

Fig. 2.— A collection of morphological properties of eight different models: (a) axisymmetric halo model with $b/a = 1.0$ and $c/a = 1.0$ (Model 2) at $T = 10.0$ ($\sim$ 2.7 Gyr), (b) no self-gravity model (Model 3, in which gaseous gravitational interaction is not included) at $T = 4.0$ ($\sim$ 1.1 Gyr), (c) Model 4 at $T = 1$ (retrograde rotation of the the triaxial halo with respect to the gas disk rotation), (d) Model 5 at $T = 6$ (higher inclination angle of the gas disk, i.e., $\theta = 60^\circ$, (e) Model 6 at $T = 4$ (more strongly barred potential in the x-y plane), (f) Model 7 at $T = 4$ (slower angular speed of $\Omega_{\rm P} = 0.77$ km s^{-1} kpc^{-1}), (g) Model 8 at $T = 4$ (faster angular speed of $\Omega_{\rm P} = 7.68$ km s^{-1} kpc^{-1}), and (h) Model 9 at $T = 4$ (compact disk with the size equal to the half of the disk of the standard model). Morphological properties are projected onto the x-y plane for Model 2, 3, 4, 6, 7, 8, and 9 and onto the x-z one for Model 5.

Table 1. Model parameters for gas disks and triaxial dark matter halos

model	$R_{\rm g}{}^a$	θ (°)	b/a	c/a	$\Omega_{\rm P}{}^b$	$R_{\rm ILR}{}^a$	$R_{\rm CR}{}^a$	$R_{\rm OLR}{}^a$	comments
1	15	30	0.8	0.6	3.84	6.8	14.2	20.7	the standard model
2	15	30	1.0	1.0	3.84	6.8	14.2	20.7	axisymmetric
3	15	30	0.8	0.6	3.84	6.8	14.2	20.7	no self-gravity
4	15	30	0.8	0.6	-3.84	-	-	-	retrograde rotation
5	15	60	0.8	0.6	3.84	6.8	14.2	20.7	more inclined disk
6	15	30	0.6	0.8	3.84	6.8	14.2	20.7	more bar-like
7	15	30	0.8	0.6	0.77	22.5	48.1	69.8	slower figure rotation
8	15	30	0.8	0.6	7.68	4.0	8.2	12.0	faster figure rotation
9	7.5	5	0.8	0.6	3.84	6.8	14.2	20.7	more compact disk

[a,b]in units of kpc and km s^{-1} kpc^{-1}, respectively

This figure "f2.jpg" is available in "jpg" format from:

http://arXiv.org/ps/astro-ph/0206208v1